Crashworthiness of Composite Structures: Modeling of the Crushing of UD Tape Sinuisoidal Specimens using a Progressive Failure Model

Presented at AMTAS Fall Meeting

Edmonds, WA - October. 2010

Francesco Deleo, Bonnie Wade, Prof. Paolo Feraboli
University of Washington

Dr. Mostafa Rassaian, Alan Byar, Mark Higgins
Boeing Research & Technology

Introduction

- *Importance of crashworthiness over “the stronger, the better” philosophy*
- *Controlled collapse ensuring safe dissipation of kinetic energy and limiting the seriousness of injuries incurred by the occupants*
- *Fiber-reinforced plastics (FRPs) can be designed to provide normalized energy absorption capabilities which are superior to those of metals*
- *Understanding prediction of the energy absorption of FRPs is not a straightforward matter*
- *FRPs are bi-phasic by nature and inherently anisotropic, their mechanical behavior is determined by a complex interpolation of a large number of variables*
- *The brittle nature of most fibers and thermosets tends to generate a <u>brittle mode of failure</u>*

Compressive Failure Mechanism: Brittle Fracture

- *Euler buckling, progressive folding, progressive crushing*
- *CFRPs typically fail by progressive crushing. Very high levels of specific energy absorption.*
- *Splaying and fragmentation failure modes*
- *The behavior of composite materials under crash conditions poses particular challenges: modeling beyond the elastic region and into failure initiation and propagation*
- *The crushing behavior of FRPs results in the interaction of failure mechanisms: matrix cracking and splitting, delamination, fiber tensile fracture and compressive kinking, frond formation and bending, and friction*
- *Current analysis methods are not capable of capturing physical behavior at the micro-level (fiber, matrix, interface) and different failure mechanisms*

Sensitivity of the model

- *Lamina-level failure criteria have been used, although with well-accepted limitations, to predict the onset of damage within laminated codes. A degradation scheme is used to reduce the material properties once failure initiated*
- *With today's computational power it is not possible to capture each of the failure mechanisms. Explicit finite element code: solves equations of motion numerically by direct integration using explicit methods*
- *Commercially available non-linear finite element packages, e.g. LS-DYNA, PAMCRASH, ABAQUS EXPLICIT, RADIOSS, are the most viable way of analyzing the crashworthiness of composite structures*
- *Commercial FEA codes use material models (or MAT cards): Progressive failure (PFM) and continuum damage mechanics (CDM) material models*
- *Each material model utilizes a different modeling strategy: failure criterion, degradation scheme, mat props, and set of parameters that are needed for computation but do not have an immediate physical meaning*
- *MAT54 is a progressive failure material model*

LS-DYNA MAT54

- *The material cards comprise material properties based on coupon-level test data*
    - *Elastic and failure (strengths, strains)*
- *Everything else is a mix of mathematical expedients, correction factors that either cannot be measured by experiment or have no direct physical meaning - these need to be calibrated by trial and error*

*MAT_054 (ENHANCED_COMPOSITE_DAMAGE)

mid	**ro**	**ea**	**eb**	**(ec)**	**prba**	**(prca)**	**(prcb)**
1	1.50E-04	8.11E+06	7.89E+06	1.00E+00	0.043	0	0
gab	**gbc**	**gca**	**(kf)**	**aopt**			
6.09E+05	6.09E+05	6.09E+05	0	3			
xp	**yp**	**zp**	**a1**	**a2**	**a3**	**mangle**	
0	0	0	0	0	0	90	
v1	**v2**	**v3**	**d1**	**d2**	**d3**	**dfailm**	**dfails**
0	0	1	0	0	0	0.013	0.03
tfail	**alph**	**soft**	**fbrt**	**ycfac**	**dfailt**	**dfailc**	**efs**
1.00E-09	0.3	0.5	0.95	1.2	0.02	-0.013	0
xc	**xt**	**yc**	**yt**	**sc**	**crit**	**beta**	
1.03E+05	1.32E+05	1.40E+05	1.12E+05	1.90E+04	54	0.5	

Material properties: elastic

Material properties: strength and strain to failure

Material Model: MAT 54

- Model is very sensitive to:
  - Filtering
  - Mesh size
  - Test speed
  - Contact definition
    - Contact type
    - LP curve
    - Trigger characteristics
  - Material model

Parameter	Baseline Value	Parametric Variation	Figure
MAT54: XT	319000	0, 5000, 50000, 150000, 250000, 300000, 350000, 370000, 400000, 500000, 640000	-
MAT54: XC	-213000	0, -100000, -150000, -200000, -230000, -250000, -265000, -275000, -300000	8
MAT54: SC	22400	1, 10000, 15000, 175000, 18000, 19000, 20000, 30000, 35000, 50000	9
MAT54: YT	7090	0, 3000, 6800, 7500, 10000, 50000, 500000	-
MAT54: YC	-28800	0, -5000, -15000, -25000, -30000, -35000, -70000, -200000, -288000, -320000, -400000, -500000	-
MAT54: DFAILT	0.0174	0, 0.005, 0.00625, 0.00688, 0.0075, 0.01, 0.015, 0.04, 0.08	10
MAT54: DFAILC	-0.0116	0, -0.005, -0.0075, -0.00813, -0.00875, -0.01, -0.012, -0.015, -0.02, -0.0225, -0.025, -0.03, -0.1	11
MAT54: DFAILM	0.024	0, 0.01, 0.015, 0.0163, 0.0165, 0.018, 0.02, 0.03, 0.06	12
MAT54: DFAILS	0.03	0, 0.006, 0.01, 0.037, 0.05, 0.1	-
MAT54: EFS	0	0.01, 0.5, 1	-
MAT54: ALPH	0.3	0, 1.00E-14, 1.00E-6, 1.00E-4, 1.00E-3, 0.03, 0.9, 1	-
MAT54: BETA	0.5	0, 1	-
MAT54: FBRT	0.5	0, 0.1, 0.95, 1	-
MAT54: YCFAC	1.2	0, 0.5, 2, 4, 7.396, 9	-
MAT54: TFAIL	0.115E-08	0, 1E-07, 0.05, 0.11	-
MAT54: SOFT	0.57	-0.5, 0, 0.05, 0.4, 0.55, 0.565, 0.575, 0.6, 0.8, 2	13
SAE Filter frequency	600	180, 1000	14
Crush Speed	150	1.5, 15, 50	15
Contact Load-Penetration Curve	PCWL	PCWL Stiff, PCWL Soft, Linear	16-19
Mesh Size	0.1	0.05, 0.15, 0.2	20, 21
Trigger Thickness	0.01	0.005, 0.015, 0.020, 0.025 0.030, 0.035, 0.040, 0.045, 0.047, 0.050, 0.060, 0.079	22
Trigger Geometry	Constant thickness	Tapered thickness	23

Feraboli, Wade, Deleo, Rassaian, Byar, and Higgins
Composites (Part A), submitted, 2010

Baseline Model

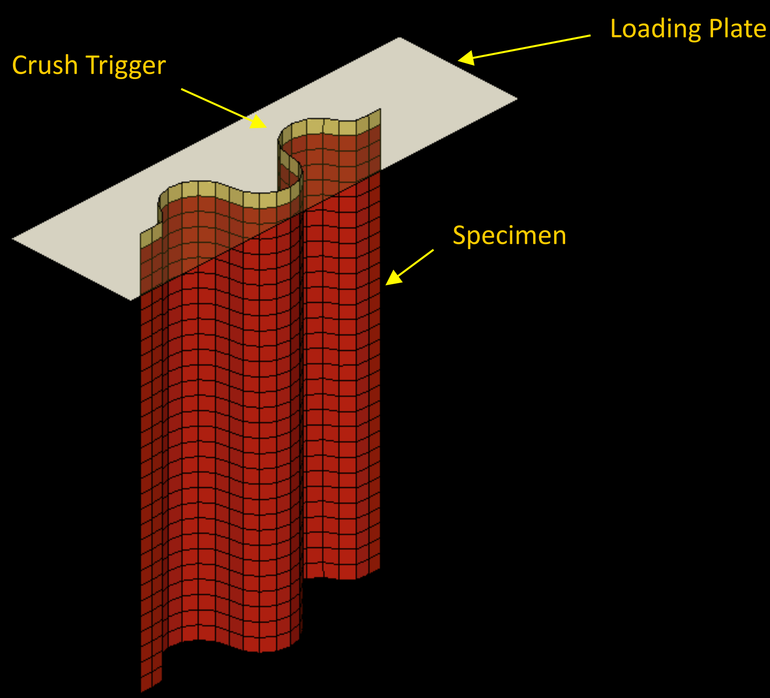

- Toray AGATE material for General Aviation
  - Toray T700 carbon fiber UD tape 12k tow
  - 2510 epoxy resin, oven cure, 270 F
- Lay-up $[(0/90)_{3S}]$, 0.079 in. thick
- 840 shell elements
- SPC Boundary conditions on bottom row of elements
- Contact Algorithm: ENTITY

Baseline Model

Property	Symbol	LS-DYNA Parameter	Experimental Value
Density	ρ	RO	0.055 lb/in³ (1.52 g/cm³)
Modulus in 1-direction	E_1	EA	18.4 Msi (127 GPa)
Modulus in 2-direction	E_2	EB	1.22 Msi (8.41 GPa)
Shear Modulus	G_{12}	GAB	0.61 Msi (4.21 GPa)
Major Poisson's ratio	ν_{12}	-	0.309
Minor Poisson's ratio	ν_{21}	PRBA	0.02049
Strength in 1-direction, tension	F_1^{tu}	XT	319 ksi (2.20 GPa)
Strength in 2-direction, tension	F_2^{tu}	YT	7.09 ksi (48. 9 MPa)
Strength in 1-direction, compression	F_1^{cu}	XC	213 ksi (1.47 GPa)
Strength in 2-direction, compression	F_2^{cu}	YC	28.8 ksi (199 MPa)
Shear Strength	F_{12}^{su}	SC	22.4 ksi (154 MPa)

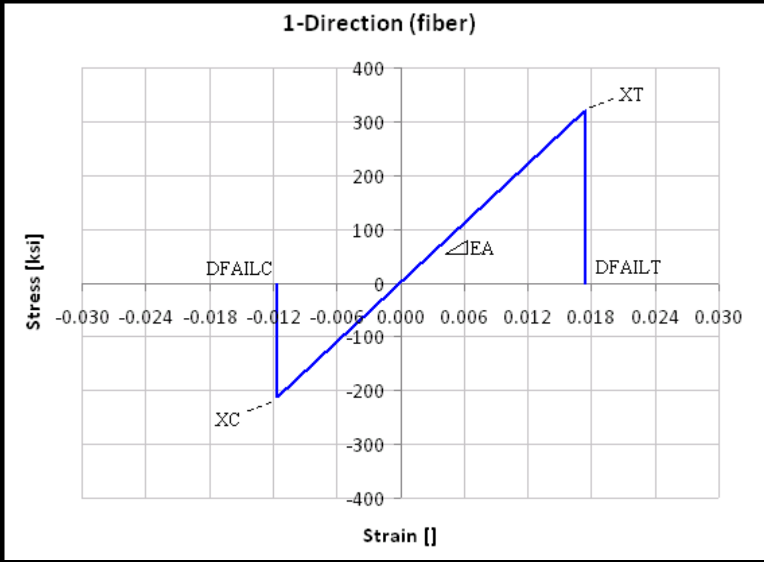

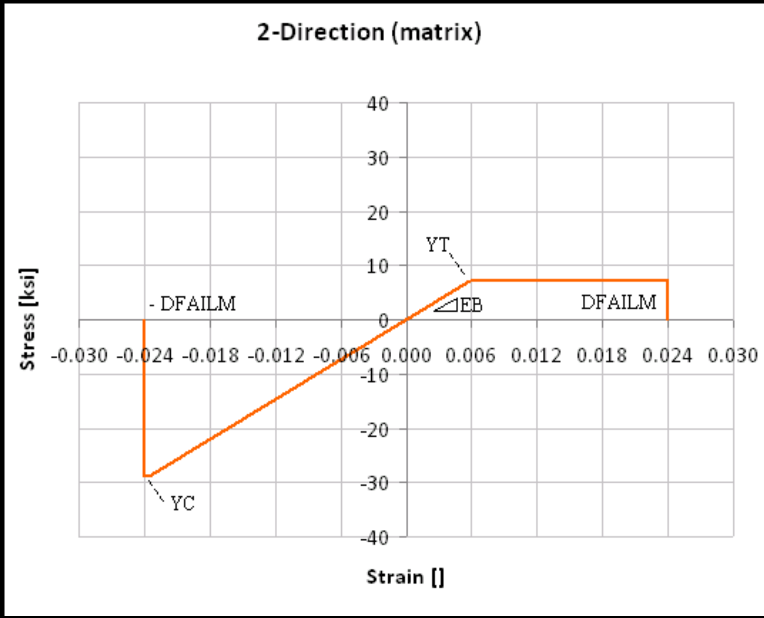

Baseline Model

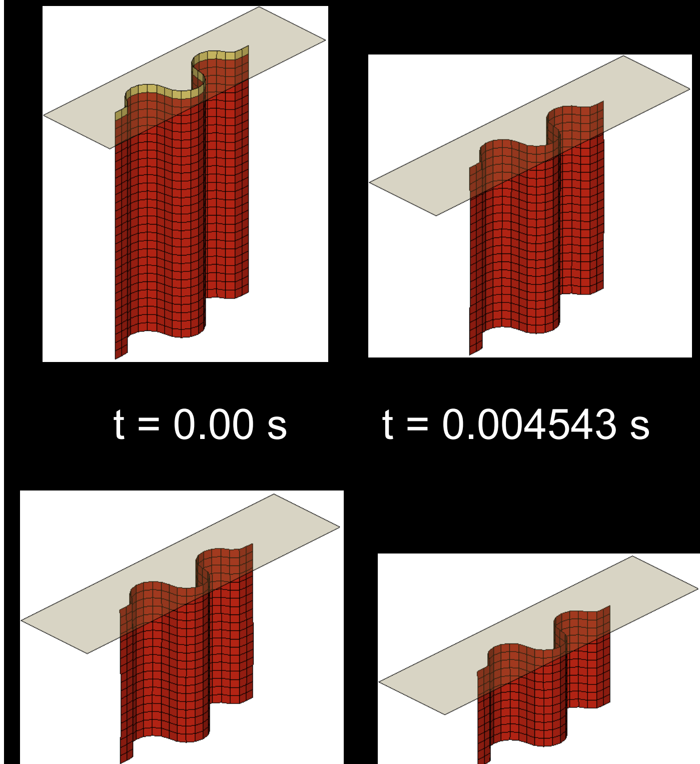

t = 0.00 s   t = 0.004543 s

t = 0.006873 s   t = 0.01153 s

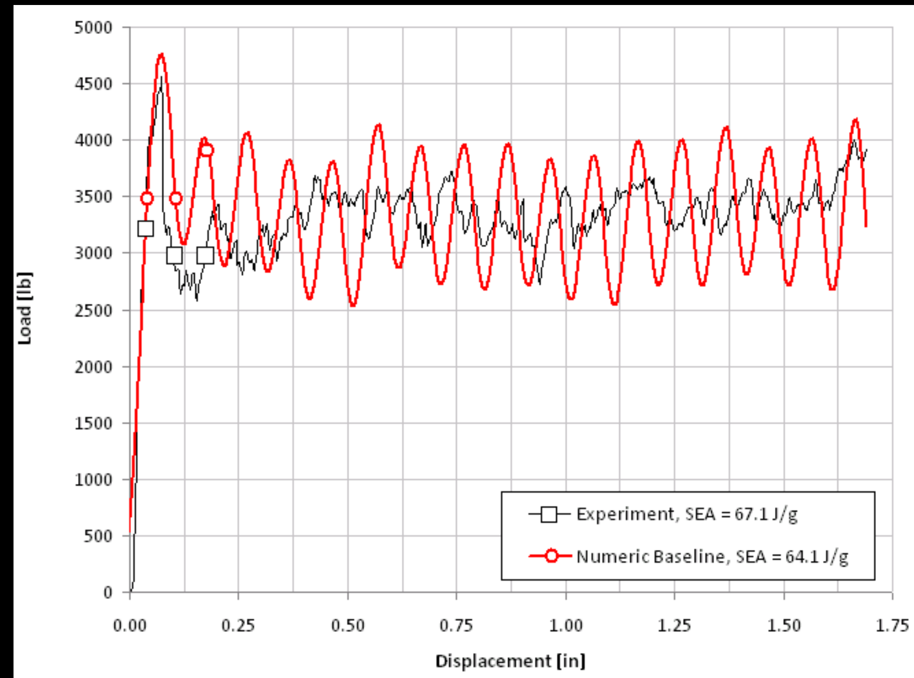

- *Obtained by inputting material properties and adjusting the control parameters, e.g SOFT, FBRT, YCFAC, and model specifics: mesh size, LP curve*
- *Failure advances in an even and stable fashion, through element deletion at the crush front*

Compressive Strength: Xc

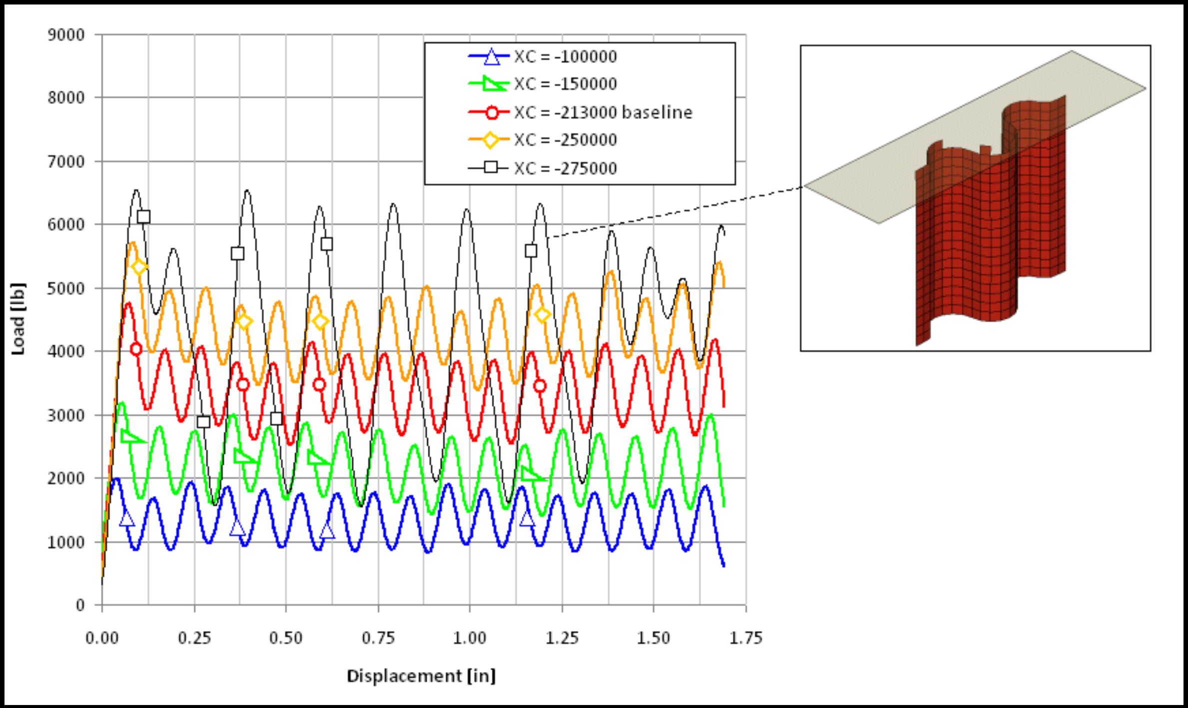

- *An effective model needs to be sufficiently robust to tolerate variations in material property input data, in order to accommodate statistical variation in measured strength and stiffness data, and yet sensitive enough to capture more significant variations*
- *Small increments in XC (Abs val) significantly lower the avg crush load and vice-versa*
- *Instability over 275 ksi compressive strength*

Shear Strength: Sc

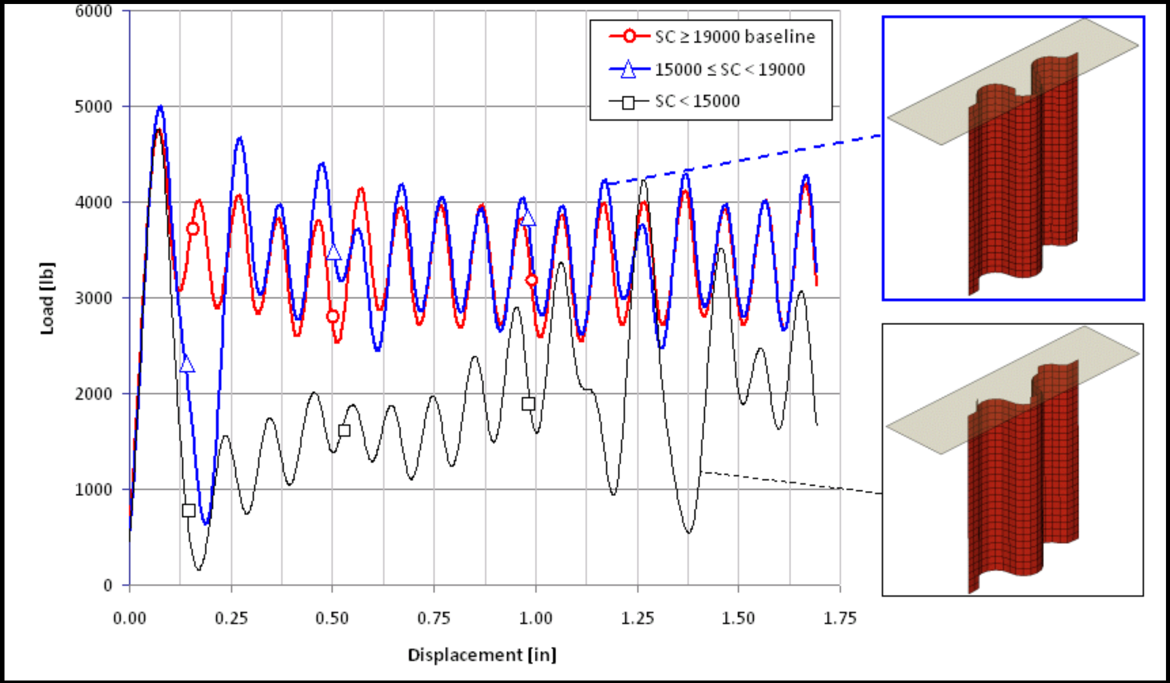

- *Unexpected and peculiar influence on stability*
- *Increasing SC does not affect the results.*
- *Decreasing SC by even 15% creates significant instabilities*
- *MAT 54 does not have a failure criterion dedicated to shear strength but SC appears to be interactive in the tensile fiber, tensile matrix, compressive matrix failure modes*
- *15% is within experimental error for shear*

Compressive Fiber Failure Strain: DFAILC

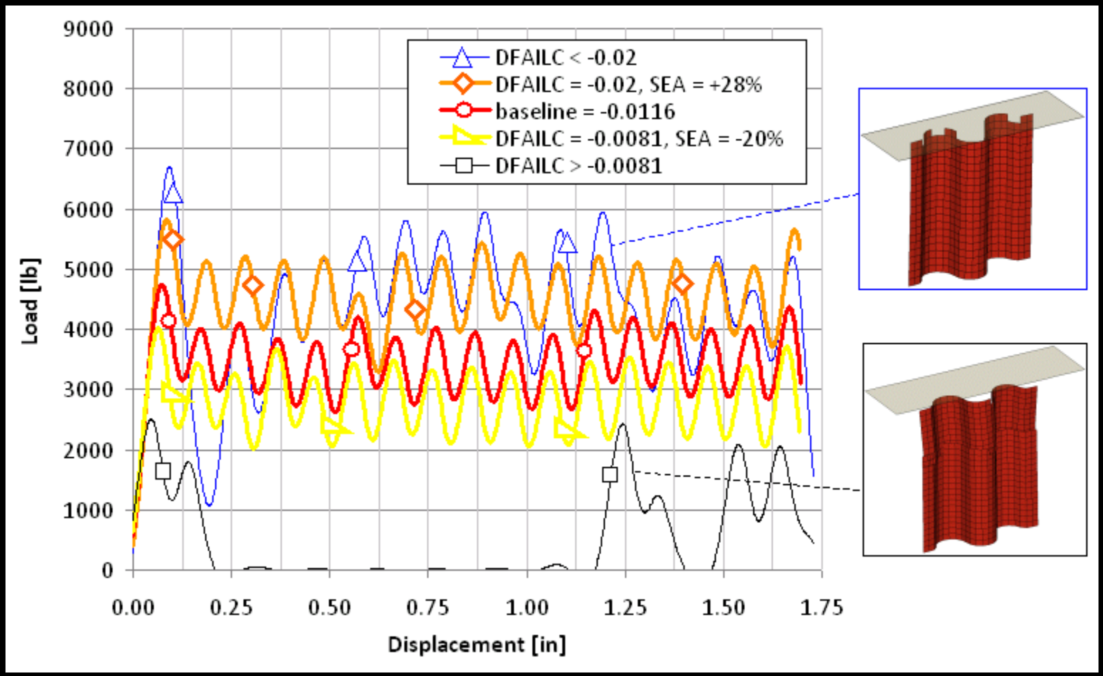

- *The compressive strain to failure has a deep effect on numerical results*
- *DFAILC = -0.02 (72% increase) results in a 28% increase in SEA, model is stable*
- *DFAILC = -0.0081 (70% decrease) results in a 20% decrease in SEA, model is stable,*
- *Higher divergences from baseline DFAILC results in numerical instabilities*

Matrix Failure Strain: DFAILM

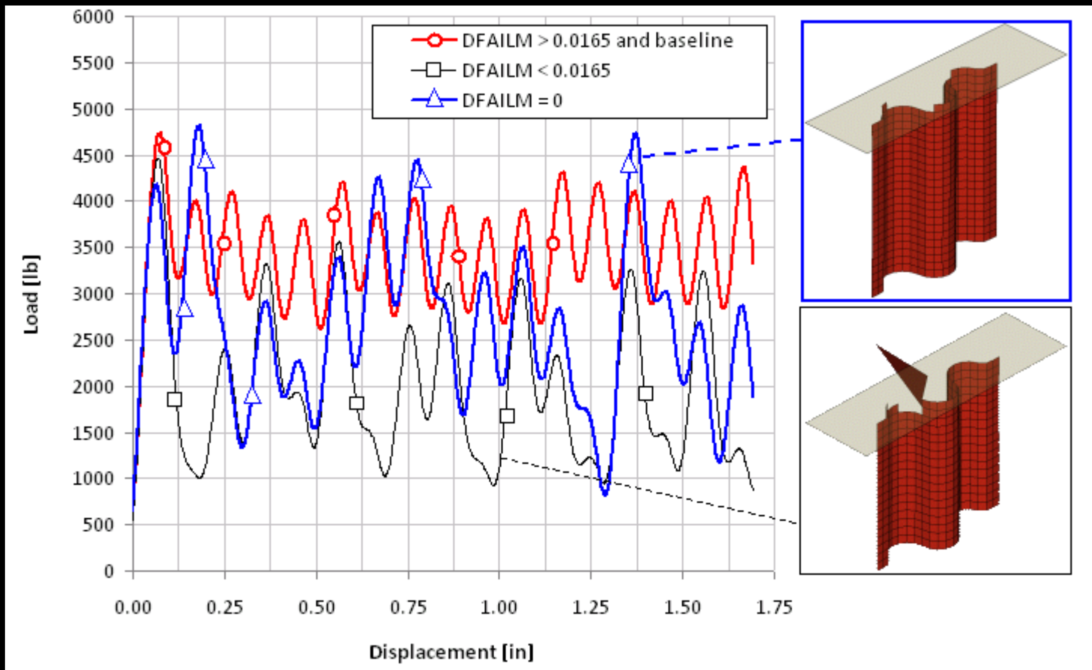

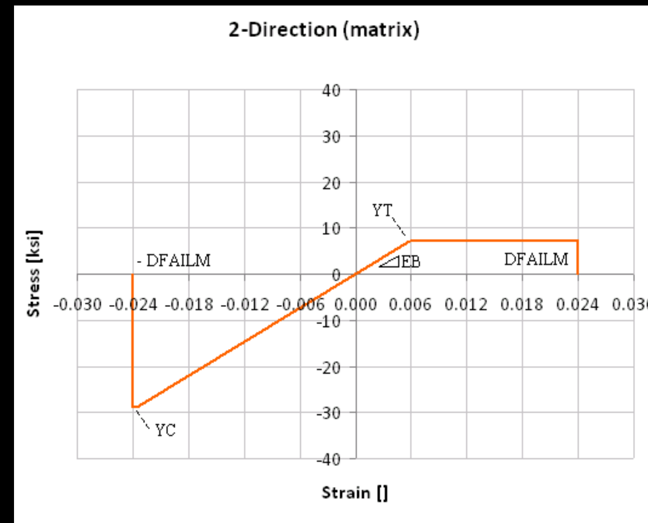

- *Zone of virtual plasticity for matrix tension*
- *BL DFAILM = 0.024*
- *Increasing DFAILM, therefore increasing perfectly plastic zone does not affect results*
- *DFAILM below 0.0165 results in model instabilities (45% change)*

Reduction Factor: SOFT

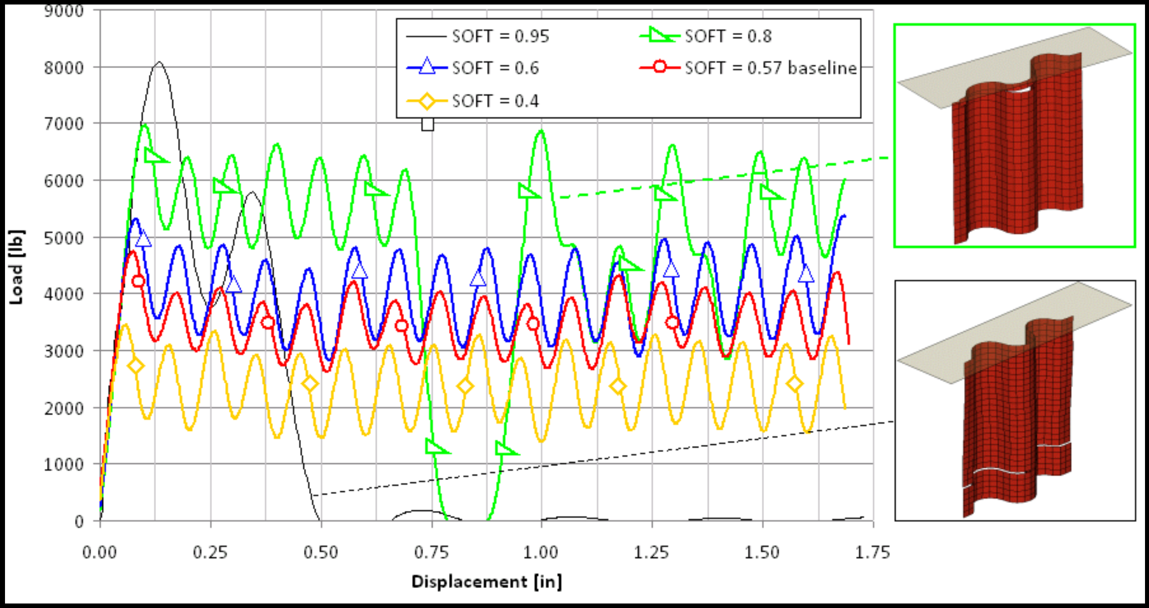

SOFT	SEA [J/g]
0.05	2.74
0.4	48.8
0.57	**64.12**
0.6	75.8
0.8	87.1
0.95	immediate buckling

- *SOFT artificially reduces the strength of the row of elements immediately ahead of the active crush front*
- *Mathematical expedient to avoid global buckling*
- *Physical interpretation: damage zone (delaminations and cracks) ahead of crush front*
- *It is the single most influential parameter in the input deck*
- *Capable of dictating whether a simulation is stable or unstable*

Contact Load Penetration Curve

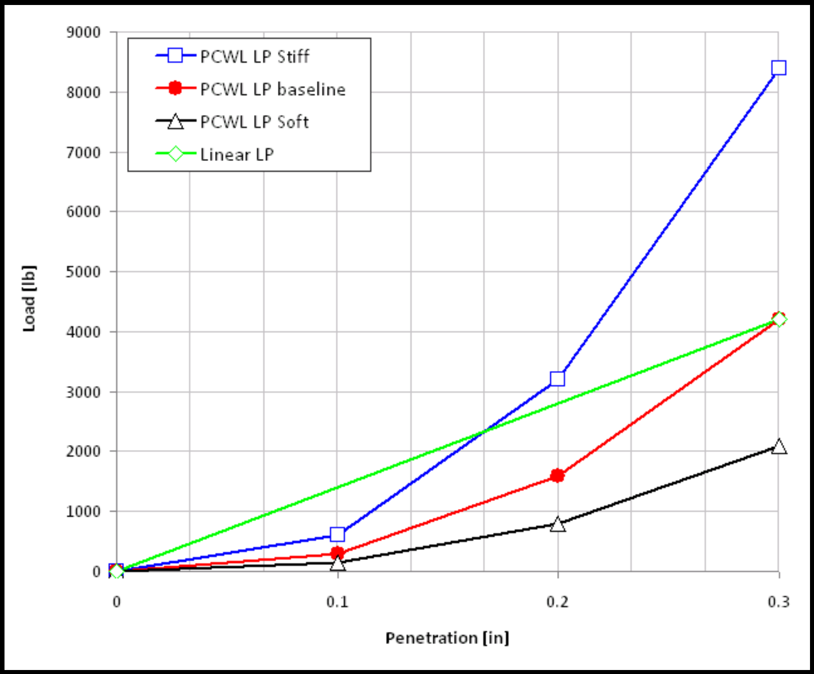

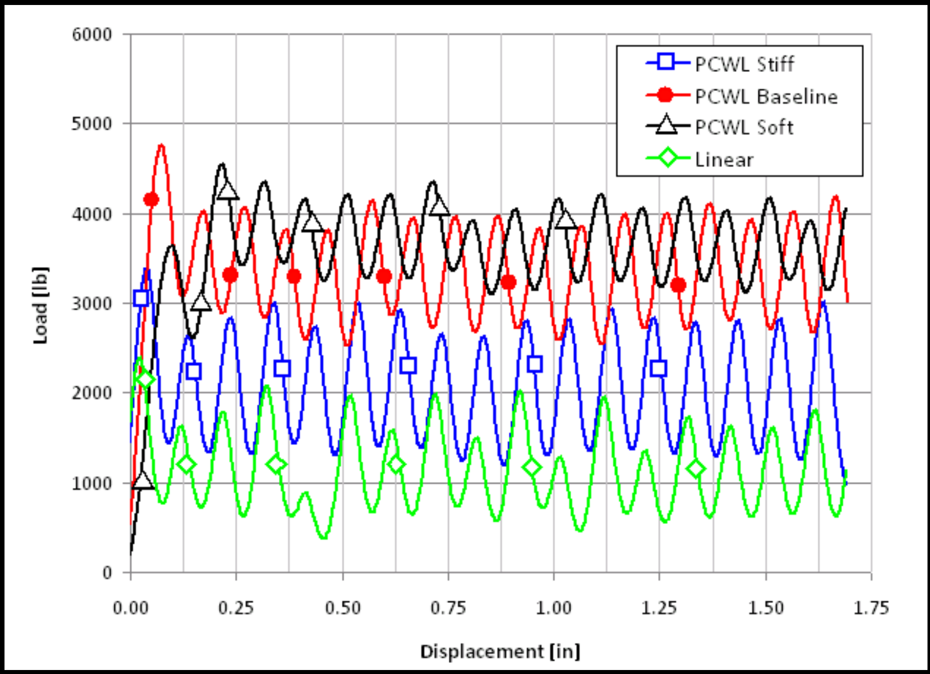

- *The LP curve has a deep effect on the numerical results*
- *There is no way of knowing a priori or determining experimentally what correct shape needs to have for specific material / geometry / loading combination*
- *Trial and error*
- *PCWL adopted for baseline*
- *Stiff LP curve: introduces load more suddenly. Soft LP curve: introduces load more gradually*

Mesh Size

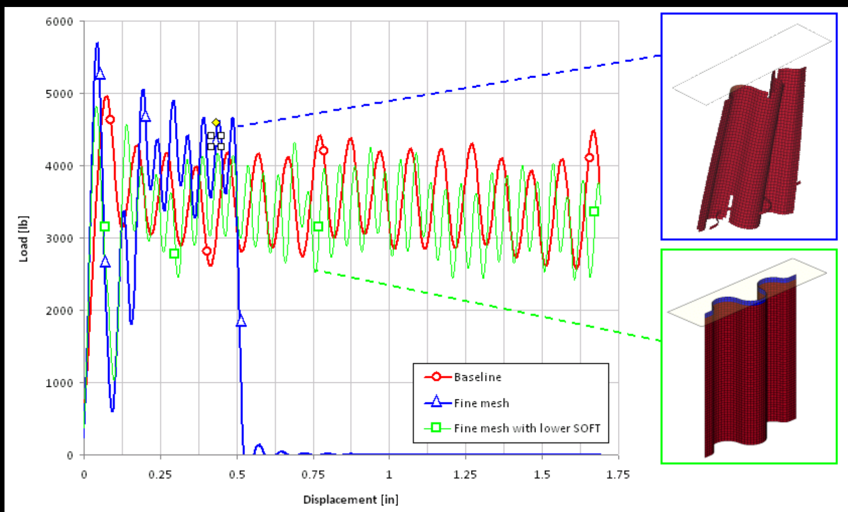

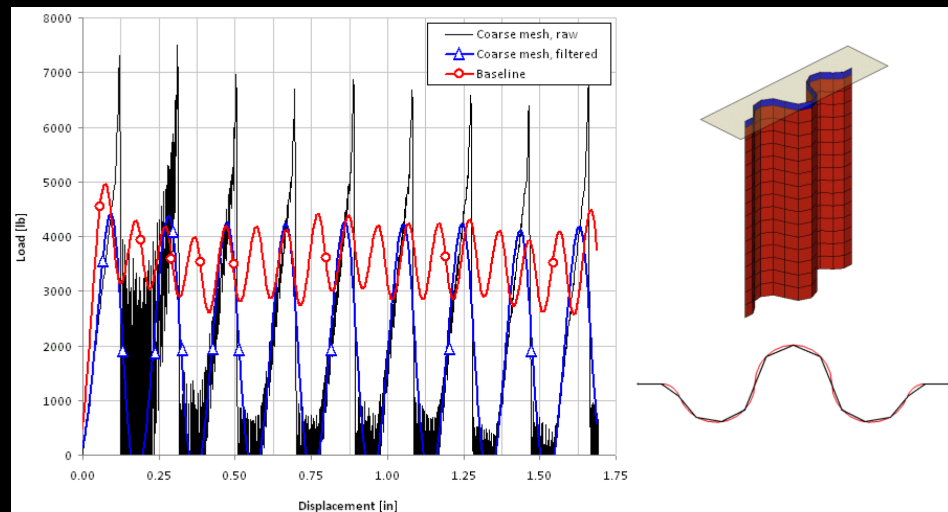

- *Coarse mesh: 0.2 in. Runtime: 43 sec. Mesh is too coarse, dead time between rows. Softening LP curve and increasing SOFT value is not sufficient to fix problem*
- *Baseline mesh: 0.1 in. Runtime: 96 sec*
- *Fine mesh: 0.05 in. Runtime: 7 min and 19 sec. With BL parameters it results in buckling. Reducing SOFT to 0.5 fixes overall stability. LP curve not able to fix initial instability*

Trigger Thickness and Geometry

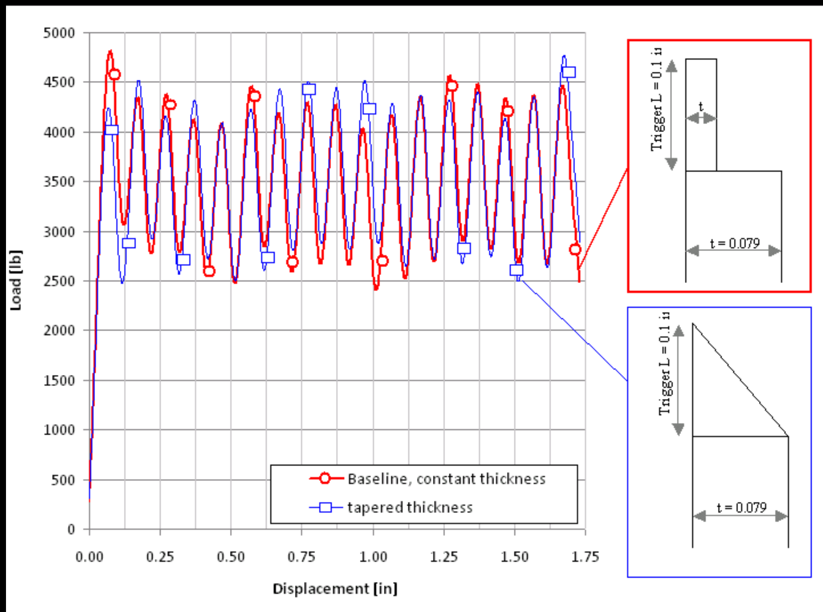

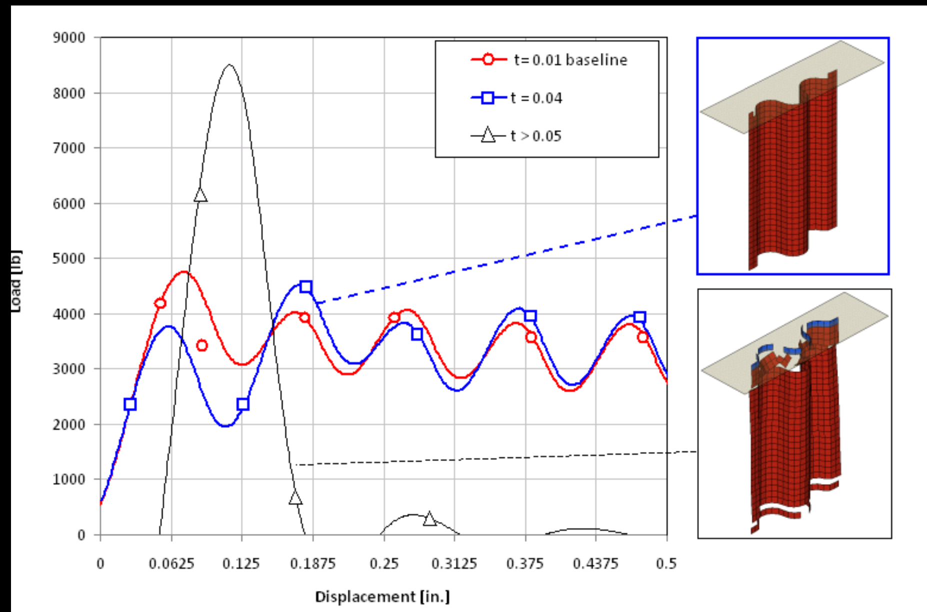

- *Crush trigger responsible for initial behavior of crushing: initial peak load and crush stability*
- *Baseline trigger: row of reduced thickness*
- *Greater thickness results in lower initial load because of filtering apparent phenomenon*
- *t > 0.05 in. results in global buckling*
- *Trigger thickness dependent of contact algortihm*
- *Tapered trigger resembles real physical trigger and has very similar global response and average crush*

Loading Speed

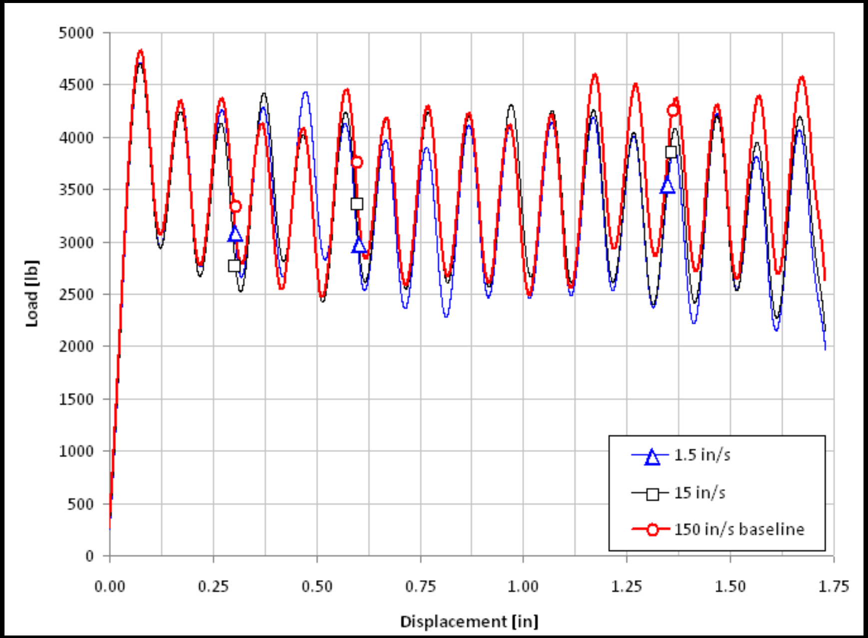

Loading rate [in/s]	Runtime [min]
1.5	164
15	16
150	1.6

- *True experimental crush loading rate is: 1.0 [in/min]*
- *To reduce experimental cost, simulations are performed at: 150 [in/s]*
- *No strain-rate dependent material properties in material card, no possible strain-rate dependent behavior*
- *Inertial effects might arise*

Multiple Baselines

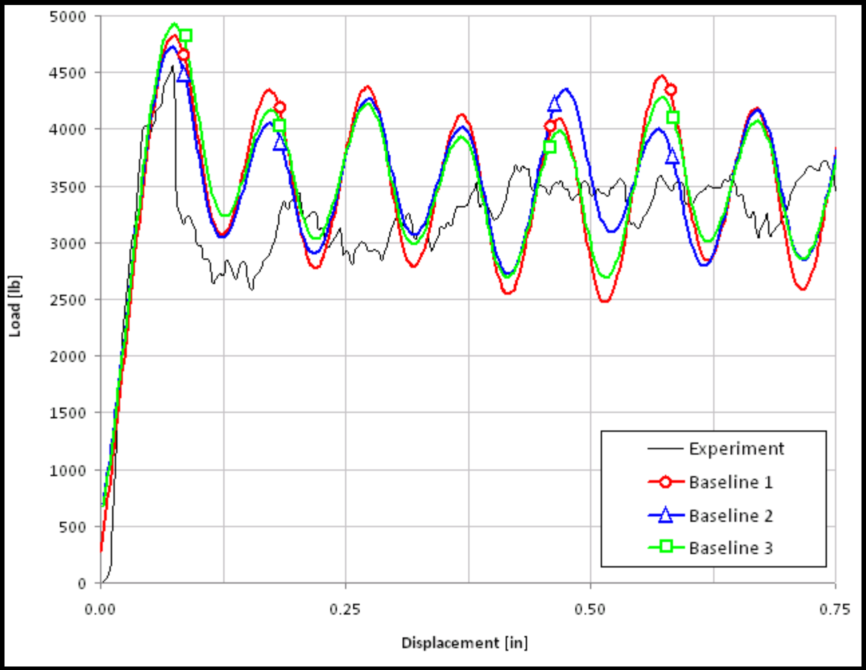

- *Varying the material properties within the experimental CoV gives rise to many different combinations of SOFT, DFAILC and XC that give excellent agreement with the experimental evidence*

Baseline	Contact Type	LP Curve	Mesh size	SOFT	DFAILC	XC	SEA [J/g]	% Error
1	Entity	PCWL baseline	0.1	0.57	-0.0116	-213,000	64.12	-4.4 %
2				0.48	-0.0175	-213,000	67.32	+0.4 %
3				0.615	-0.0100	-213,000	67.80	+1.1 %
4				0.62	-0.0116	-200,000	66.39	-1.0%
5				0.54	-0.0116	-230,000	66.49	-0.9%

Conclusions

- *Current modeling approach with LS-DYNA MAT54 is not predictive at this structural level (element)*
- *The simulation can be matched to the experiment but cannot predict it*
- *Through proper calibration at the coupon and element level, it is possible however to use the model to predict the behavior of higher structural levels (subcomponent and full-scale)*
- *The parameters: XC, SC, DFAILC, DFAILM were found to have a significant effect on the numerical results*
- *SOFT and contact definition (LP curve in particular) gave dramatic effects on results of simulations. Yet they cannot be determined a priori but only calibrated to match experiment*
- *Varying the loading speed was found to not have a significant effect on the numerical results*

References

- Carruthers, J.J., Kettle, A.P. and Robinson, A.M., "Energy Absorption Capability and Crashworthiness of Composite Material Structures: A Review", Applied Mechanics Reviews, 51, 1998, pp. 635-649.
- Farley, G.L., Jones, R.M., “Crushing characteristics of continuous fiber-reinforced composite tubes”, Journal of Composite Materials, 26/1, 1992, pp. 37–50.
- Hull D (1991), A unified approach to progressive crushing of fibre-reinforced composite tubes, *Composites Sci Tech*, 40, 377-421
- Hinton, M.J., Kaddour, A.S., Soden, P.D., “A comparison of the predictive capabilities of current failure theories for composite laminates, judged against experimental evidence”, Composites Science and Technology, 62/ 12-13, 2002, pp. 1725-1797.
- Xiao, X., “Modeling Energy Absorption with a Damage Mechanics Based Composite Material Model”, Journal of Composite Materials, March 2009; vol. 43/ 5, 2009, pp. 427-444.
- Feraboli, P., Rassaian, M., “Proceedings of the CMH-17 (MIL-HDBK-17) Crashworthiness Working Group Numerical Round Robin”, Costa Mesa, CA, July 2010.
- Hallquist, J.O., “LS-DYNA Theoretical Manual”, Livermore Software Technology Corporation, 2005.
- Feraboli P., “Development of a corrugated test specimen for composite materials energy absorption”, Journal of Composite Materials - 42/3, 2008, pp. 229-256.
- Feraboli P., “Development of a modified flat plate test and fixture specimen for composite materials crush energy absorption”, Journal of Composite Materials, 43/19, 2009, pp. 1967-1990.
- Feraboli P., Norris C., McLarty D., “Design and certification of a composite thin-walled structure for energy absorption”, International Journal of Vehicle Design, Vol. 44/ 3-4, 2007, pp. 15-36
- Tomblin, J., Sherraden, J., Seneviratne, W., Raju, K.S., “A-basis and B-basis Design Allowables for Epoxy-based prepreg Toray T700SC-12K-50C/ #2510 Plain Weave Fabric”, AGATE-WP3.3-033051-131, Sept. 2002.
- “T700SC 12K/ 2510 Plain Weave Fabric”, Composite Materials Handbook (CMH-17), Volume 2, Chapter 4.2.38, Rev. G.
- Browne, A.L., Johnson, N.L., “Dynamic axial crush of automotive rail sized composite tubes, Part 5: Effect of test conditions”, American Society for Composites (ASC), 18th Annual Technical Conference, Paper 152, September 2003, Gainesville, FL.
- Chang FK, Chang KY, A Progressive Damage Model for Laminated Composites Containing Stress Concentration, J Composite Materials, 21, 1987, 834-855.
- Feraboli P., Deleo F., Wade B., Rassaian M., Higgins M., Byar A., Reggiani M., Bonfatti A., DeOto L., Masini A., “Predictive modeling of an energy-absorbing sandwich structural concept using the building block approach”, Composites (Part A), 41/6, 2010, pp. 774-786
- Fasanella, E.L., Jackson, K.E., “Best practices for crash modeling simulation”, NASA TM-2002-211944, ARL-TR-2849, October 2002.
- Feraboli, P., Wade, B., Deleo, F., Rassaian, M., “Crush energy absorption of composite channel section specimens”, Composites (Part A), 40/8, 2009, pp. 1248-1256.
- Paz M, Structural Dynamics Theory and Computation, 3rd edition, Van Nostrand Reinhold, New York, 1991.
- Meyer C, Will KM, Models for Dynamic Analysis in Finite Element Idealization, American Society of Civil Engineers, New York, 1987.
- Zukas JA, Nicholas T, Swift HF, Greszczuk LB, Curran DR, Impact Dynamics, John Wiley & Sons, 1982.

APPENDIX: Brittle Fracture

- *Progressive Crushing: CFRPs and GFRPs typically fail by this mechanisms. Very high levels of energy absorption. Serrations: stresses required to initiate crack growth are higher than those for propagation.*
- *Splaying crushing mode: very long interlaminar, intralaminar, and parallel to fiber cracks. Little or none fracture of axial laminar bundles. Crack growth is the principal energy absorption mechanism [Hull].*

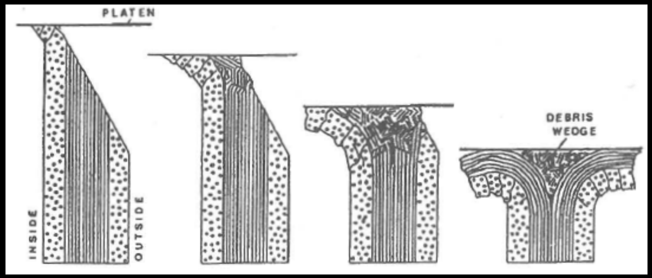

- *Fragmentation crushing mode: wedge-shaped laminate cross section. Short interlaminar and longitudinal cracks forming partial lamina bundles. Fracture of the lamina bundles is the primary energy absorption mechanism [Hull].*

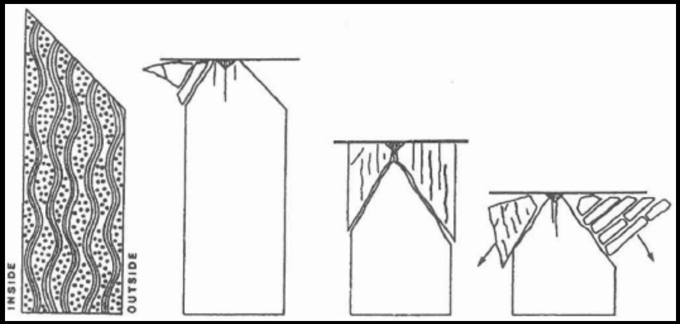

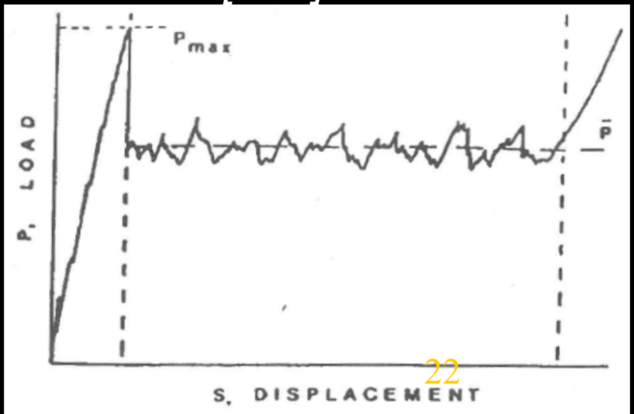

Appendix: MAT 54 Failure Criteria

- *For the tensile fiber mode where σ11>0:*

$$e_f^{\,2} = \left(\frac{\sigma_{11}}{F_1^{\,tu}}\right)^2 + \beta\left(\frac{\sigma_{12}}{F_{12}^{\,su}}\right)^2 \begin{cases} \geq 1 \; failed \\ < 1 \; elastic \end{cases}$$

Upon failure: E1 = E2 = G12 = v12 = v21 = 0

For BETA = 1 the Hashin failure criterion is implemented, while setting BETA = 0 reduces to the Maximum Stress failure criterion.

- *For the compressive fiber mode where σ11<0:*

$$e_c^{\,2} = \left(\frac{\sigma_{11}}{F_1^{\,cu}}\right)^2 \begin{cases} \geq 1 \; failed \\ < 1 \; elastic \end{cases}$$

Upon failure: E1 = v12 = v21 = 0

- *For the tensile matrix mode where σ22>0:*

$$e_m^{\,2} = \left(\frac{\sigma_{22}}{F_2^{\,tu}}\right)^2 + \left(\frac{\sigma_{12}}{F_{12}^{\,su}}\right)^2 \begin{cases} \geq 1 \; failed \\ < 1 \; elastic \end{cases}$$

Upon failure: E2 = v21 = G12 = 0

- *For the compressive matrix mode where σ22<0:*

$$e_d^{\,2} = \left(\frac{\sigma_{22}}{2F_{12}^{\,su}}\right)^2 + \left[\left(\frac{F_2^{\,cu}}{2F_{12}^{\,su}}\right)^2 - 1\right]\frac{\sigma_{22}}{F_2^{\,cu}} + \left(\frac{\sigma_{12}}{F_{12}^{\,su}}\right)^2 \begin{cases} \geq 1 \; failed \\ < 1 \; elastic \end{cases}$$

Upon failure: E2 = v21 = v12 = 0 = G12 = 0

Beside strength-based criteria, failure can also occur if the strains exceed the strain to failure for each ply. Element deletion can also occur is the element time step TFAIL is exceeded.

Appendix: FBRT and YCFAC

- Matrix failure corresponds to first ply failure . The FBRT and YCFAC strength reduction parameters are used to degrade the pristine fiber strengths of the remaining plies once matrix failure takes place

$$XT = XT^* * FBRT$$

$$XC = YC^* * YCFAC$$

- The FBRT factor acts as a percentage reduction of the tensile fiber strength from its pristine value, therefore its value may only be in the range [0, 1]. The YCFAC factor uses the pristine matrix strength YC to determine the damaged compressive fiber strength [0, 7.4]
- The input value for the two parameters FBRT and YCFAC cannot be measured experimentally and need to be determined by trial and error
- First ply failure is in the tensile matrix mode. The FBRT & YCFAC strength reduction parameters are active after compressive matrix failure
- Results show that the simulation is unaffected by the fiber strength degradation scheme. These factors have negligible effect on the results of the simulation

Appendix: TFAIL

- The simulation runs unaffected for small values of TFAIL, such as [1E-08, 1E-05]
- Using TFAIL = 0 leads to immediate global buckling because of the SOFT condition violation
- Using large TFAIL values in the range [0.001, 0.1] should be avoided, since the time-step of the simulation is smaller and elements are deleted before being loaded
- It should be emphasized that LS-DYNA assigns the time-step automatically to ensure that the Courant condition is satisfied. In this case the default time-step is 2.44219 E-7
- Courant Condition: $$\Delta t = \frac{k\Delta h}{c}$$
  - Where, Δt is the time step, Δh is the characteristic mesh dimension, k is a stability factor (0.6 – 0.8), and c is the speed of the sound wave through the material